Multispectral mid-infrared light emitting diodes on a GaAs substrate

Mohsin Aziz, Chengzhi Xie, Vincenzo Pusino, Ata Khalid, Matthew Steer, Iain G. Thayne, and David R. S. Cumming

Citation: Appl. Phys. Lett. **111**, 102102 (2017); doi: 10.1063/1.4986396
View online: http://dx.doi.org/10.1063/1.4986396
View Table of Contents: http://aip.scitation.org/toc/apl/111/10
Published by the American Institute of Physics

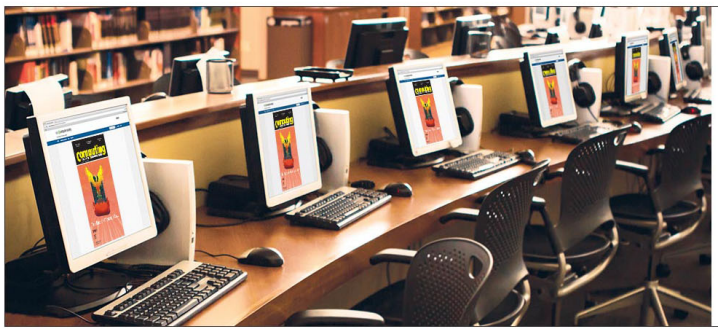

Multispectral mid-infrared light emitting diodes on a GaAs substrate

Mohsin Aziz, Chengzhi Xie, Vincenzo Pusino, Ata Khalid,[a] Matthew Steer, Iain G. Thayne, and David R. S. Cumming
Electronics and Nanoscale Division, School of Engineering, University of Glasgow, Glasgow G12 8LT, United Kingdom

(Received 5 June 2017; accepted 21 August 2017; published online 5 September 2017)

We have designed, simulated, and experimentally demonstrated four-colour mid-infrared (mid-IR) Light Emitting Diodes (LEDs) integrated monolithically into a vertical structure on a semi-insulating GaAs substrate. In order to finely control the peak wavelength of the emitted mid-IR light, quantum well (QW) structures based on AlInSb/InSb/AlInSb are employed. The completed device structure consists of three p-QW-n diodes with different well widths stacked on top of one bulk AlInSb p-i-n diode. The epitaxial layers comprising the device are designed in such a way that one contact layer is shared between two LEDs. The design of the heterostructure realising the multispectral LEDs was aided by numerical modelling, and good agreement is observed between the simulated and experimental results. Electro-Luminescence measurements, carried out at room temperature, confirm that the emission of each LED peaks at a different wavelength. Peak wavelengths of 3.40 μm, 3.50 μm, 3.95 μm, and 4.18 μm are observed in the bulk, 2 nm, 4 nm, and 6 nm quantum well LEDs, respectively. Under zero bias, Fourier Transform Infrared photo-response measurements indicate that these fabricated diodes can also be operated as mid-IR photodetectors with an extended cut-off wavelength up to 4.6 μm. [http://dx.doi.org/10.1063/1.4986396]

In the infrared absorption band, Mid-infrared (mid-IR) radiation with wavelengths between 2 and 5 μm can be exploited for many applications, such as gas sensing (e.g., for sensing CO, CO_2, and CH_4), process monitoring, and biological molecule detection and imaging. Single-wavelength Mid-IR emitting Light Emitting Diodes (LEDs) based on various technologies have been demonstrated and often commercialised;[1] however, a cost-effective technology able to deliver multi-spectral mid-IR LEDs with good performance has not yet emerged. Monolithically integrated two-colour devices have been reported on the same chip in the visible spectral range.[2] Similar work has reported bi-colour devices in the infrared range.[3–5] Jung has demonstrated two-wavelength tunable mid-IR LEDs grown on a GaSb substrate,[4] which are based on bottom (GaSb substrate) emission. Such schemes have two major disadvantages: first is the use of a GaSb substrate, which is not available in large formats compared to Si and GaAs; second, mechanical polishing and thinning of the substrate are required. Das[6] has reported dual-colour devices in the mid-IR and in the Long Wave InfraRed (LWIR) range, also using a GaSb substrate. In this study, we have grown four different mid-IR LEDs on a Semi-Insulating (SI) GaAs substrate. These devices exploit the variation of the quantum well width to induce a change in the localisation of the quantized energy levels within the well and thus produce three different wavelengths in the mid-IR range. Previous studies[7–9] showed that InSb p-i-n mid-IR detectors grown on GaAs substrates were integrated and addressed through underlying GaAs MESFETs. Functionalisation of the bottom GaAs layers for switching and addressing the multispectral LEDs has potential to deliver cost-effective monolithically integrated arrays of mid-IR LEDs at multiple wavelengths, without resorting to costly, low-yield hybrid flipped chip techniques.[10] In this letter, we report four monolithically integrated Mid-IR LEDs, each emitting at a different peak wavelength. The emission of three LEDs is based on emission from a quantum well (QW) heterostructure, whereas the fourth LED is based on a bulk p-i-n structure which has been previously reported.[7–9]

The layer structure of the material used to fabricate the LEDs is shown in Fig. 1(a). It can be seen from the layer structure that the LEDs are designed in such a way that two devices share at least one contact layer between them. This is to facilitate the electrical switching of each LED independently. The three QW-based LEDs have quantum wells whose widths are 2 nm, 4 nm, and 6 nm. The epitaxial layers were grown on a 3″ SI GaAs wafer using a Veeco Gen III Molecular Beam Epitaxy (MBE) system equipped with arsenic and antimony valved cracker sources. Te and Be were used for the n and p-type dopants, respectively, in the Antimonide containing layers of the device. The growth started with GaAs buffer layers at 590 °C; the temperature was then lowered, and an intermediate buffer layer of GaSb was grown at 500 °C. For the growth of GaSb on GaAs, Interfacial misfit (IMF) growth conditions were used which favour the relief of strain between GaAs and GaSb by misfit dislocations at the interface.[11,12] This IMF technique significantly reduces the number of threading dislocations which propagate through the layer vertically.[12] Subsequently, the temperature was lowered down to 400 °C and 50 nm of AlInSb were grown. The temperature was then raised by

[a]Author to whom correspondence should be addressed: ata.khalid@glasgow.ac.uk

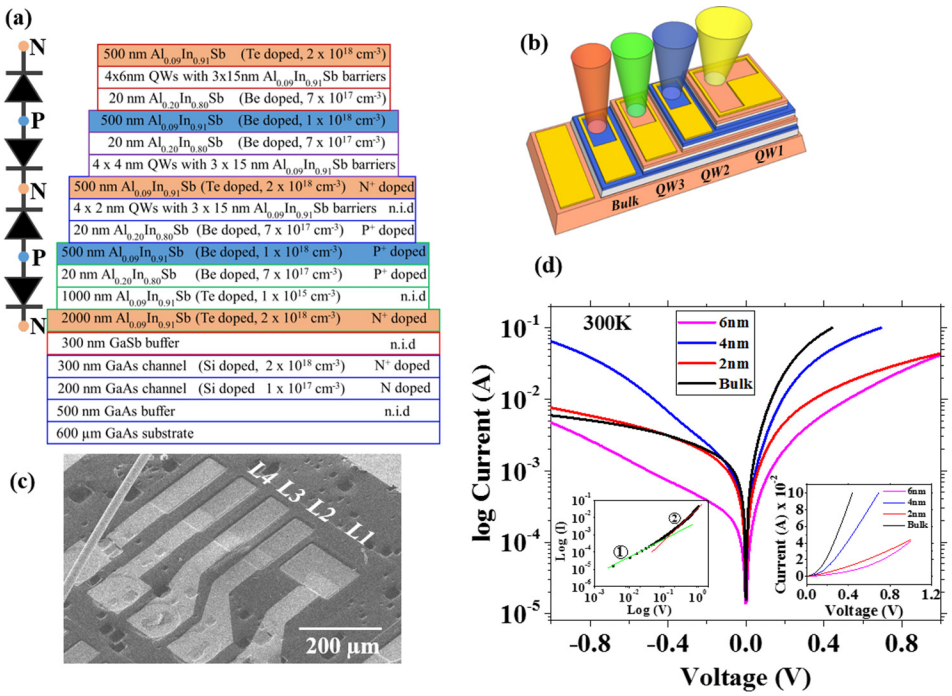

FIG. 1. (a) Layer structure design of LEDs, (b) a 3D schematic of fabricated LEDs, (c) the SEM of final fabricated devices, and (d) current-Voltage measurements of all LEDs at room temperature; the two insets show log-log (I-V) where two regions are apparent and linear forward Voltage-Current.

50 °C, and the remainder of the bulk LED device and MQW layers were grown at ~450 °C.

The LEDs were fabricated using standard photolithography and wet etching techniques. Citric acid etchant [citric acid: H_2O_2:H_2O, (11:1:7)] was used to etch individual LEDs up to 2000 nm before deposition of the metal Ohmic contacts. The top contact of each LED has an optical window for light emission. The side-walls of the devices were passivated with silicon nitride (SiN_x) and polyimide to minimise surface recombination current and associated leakage. Polyimide was also used to planarise the surface obtained after the multiple wet etches and facilitate a smooth interconnection between the electrodes of the LEDs and the probe and bonding pads on the SI GaAs. A 3D schematic of the LEDs is shown in Fig. 1(b). A Scanning Electron Micrograph (SEM) image of the completed device is shown in Fig. 1(c). The defects visible on the surface around the mesas of the fabricated devices are associated with threading dislocations and defects due to the lattice mismatch at the GaAs-GaSb interface. These defects were exposed after the wet etching of ~7.5 μm Antimonide material to reach the SI GaAs where all probe contact pads were deposited.

The IV characterisation of all of the LEDs was carried out by using an Agilent B201A current source, and the IV curves for all four LEDs are shown in Fig. 1(d). Two important parameters, ideality factor and series resistance, were extracted using the Werner method,[13] and their values are summarised in Table I. The LEDs with quantum-well widths of 6 nm and 2 nm show lower values of the ideality factor but higher series resistance values. The lower values of the ideality factor in 2 nm and 6 nm Quantum well LEDs are associated with the lower value of leakage current. Among all four LEDs, the 2 nm and 6 nm quantum well LEDs show lowest dark current and hence have lower ideality factors. The log-log scale of current-voltage indicates two regions, labelled 1 and 2 in the left inset of Fig. 1(d). At a small forward bias, the lower ideality factor value indicates the competition mechanism of drift-diffusion and the recombination process. At a larger forward bias, higher than 0.15 V, the current is mainly limited by the series resistances effect.

TABLE I. LED parameters extracted using the Werner Method.[13]

Parameters	Bulk	2 nm	4 nm	6 nm
Ideality factor	1.31	1.22	1.25	1.12
Series resistance (Ω)	2.2	27	3	77

The emission from the quantum wells can be tuned by varying the well width. The emission band shifts to higher energies by decreasing the well width.[14–16] The effects of such localisation-induced emission are simulated using the software SiLENSe. Initially, the simulation has been done on LEDs with a range of quantum well widths. The peak of the emission wavelength can be tuned by changing the well width. The quantum well widths of 2 nm, 4 nm, 6 nm, 8 nm, and 10 nm show peak emission at 3.7 μm, 4.0 μm, 4.3 μm, 4.6 μm, and 4.8 μm, respectively, as shown in Fig. 2(a). Figure 2(b) illustrates a typical energy band diagram of devices with quantum wells and electron blocking barrier.

The LEDs were measured with a Bruker Vertex70 Fourier Transform Infrared (FTIR) spectrometer, equipped with a cooled InSb detector. An external pulsed current generator was used to drive the LEDs, setting the duty cycle to 50% in order to avoid Joule heating of devices. All LEDs were mounted on a 28-pin ceramic leadless chip carrier (LCC) and wire bonded in order to be measured. Figures 3(a) and 3(b) show the comparison of Electro-Luminescence (EL) spectra of four LEDs, namely, bulk, 2 nm, 4 nm, and 6 nm. In the 6 nm LED, the sudden dip in emission appearing at 4.2 μm is due to the absorption caused by atmospheric CO_2, since these LEDs are measured at ambient conditions. The spectra shown were collected at 20 mA forward current for all four devices. The peak of the EL spectrum shifts to a higher wavelength from the bulk to the quantum well LEDs.

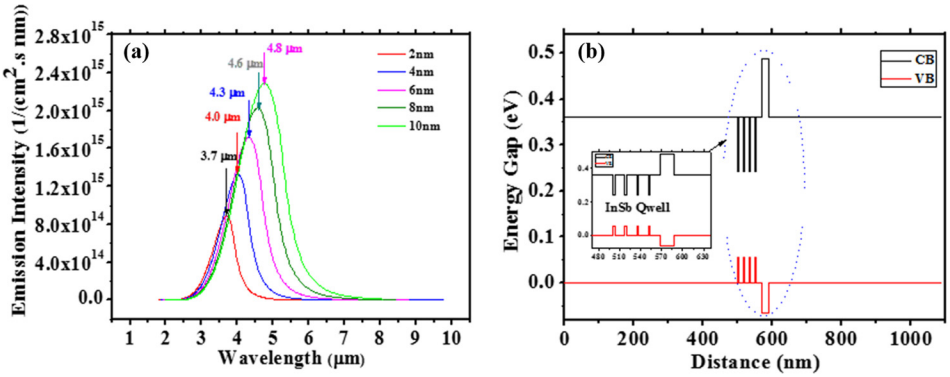

FIG. 2. (a) Simulated LED Under Test (LUT) spectra with varying quantum well widths and (b) energy band diagram of the AlInSb/InSb/AlInSb quantum well with the AlInSb electron blocking barrier.

This indicates the tunability of the wavelength of peak emission from 3.40 μm to 4.18 μm. Table II compares the experimental results with the simulated emission wavelengths of the three quantum-well LEDs: a good agreement can be observed for all three devices. The LEDs were also measured at zero bias to investigate the photocurrent spectra of the LEDs and assess the possibility of using them as mid-IR detectors. The same FTIR spectrometer (Bruker Vertex 70) was used to measure the relative photo-response from each device (2 nm, 4 nm, 6 nm quantum well, and bulk p-i-n LEDs). The photo-response measurements were carried out at room temperature and standard atmosphere with no bias voltage. The photo-response was detected using a current preamplifier connected to the N-doped side of LEDs, and the response from each device was collected so that only the p and n contacts of a single device were connected, while the rest of the devices were under floating conditions. As it can be seen from Figs. 3(c) and 3(d), the photo-response of the devices covers the range from the Near InfraRed (NIR) to the mid-IR. The cut off wavelength of the devices showed a similar trend to the peak-wavelengths of the EL spectra [Fig. 3(d)] and varied according to the designed structure. The FTIR photo response was measured at zero bias, indicating that a photocurrent mechanism exists with these devices. The distinct threshold of absorption is observed to be below the bandgap of the $Al_{0.2}In_{0.8}Sb$ barrier material indicating absorption directly into the confined levels within the individual quantum wells. The light absorption in the Quantum Wells is expected to be limited due to the small number of quantum wells; nevertheless, absorption into a quantum well is expected to be higher than the bulk material of a similar thickness due to the increased density of states known to exist in low dimensional structures. In order that these confined photo-generated carriers contribute to the observed photocurrent, a mechanism for excitation into the barrier material must exist; a possible mechanism for this could be due thermal excitation of the confined carriers from the quantum wells into states above or close to the barrier allowing the photocurrent to be detected.[17]

The dependence of the emission from all LEDs on the forward injection current is shown in Fig. 4. The LEDs showed either a blue shift, a mixture of blue and redshift, or a consistent red shift in wavelength with the increase in the input injection current. The 2 nm quantum well based LED showed a decrease in the wavelength from 3.489 μm to 3.484 μm (blue-shift of 50 nm). The 4 nm LED showed a

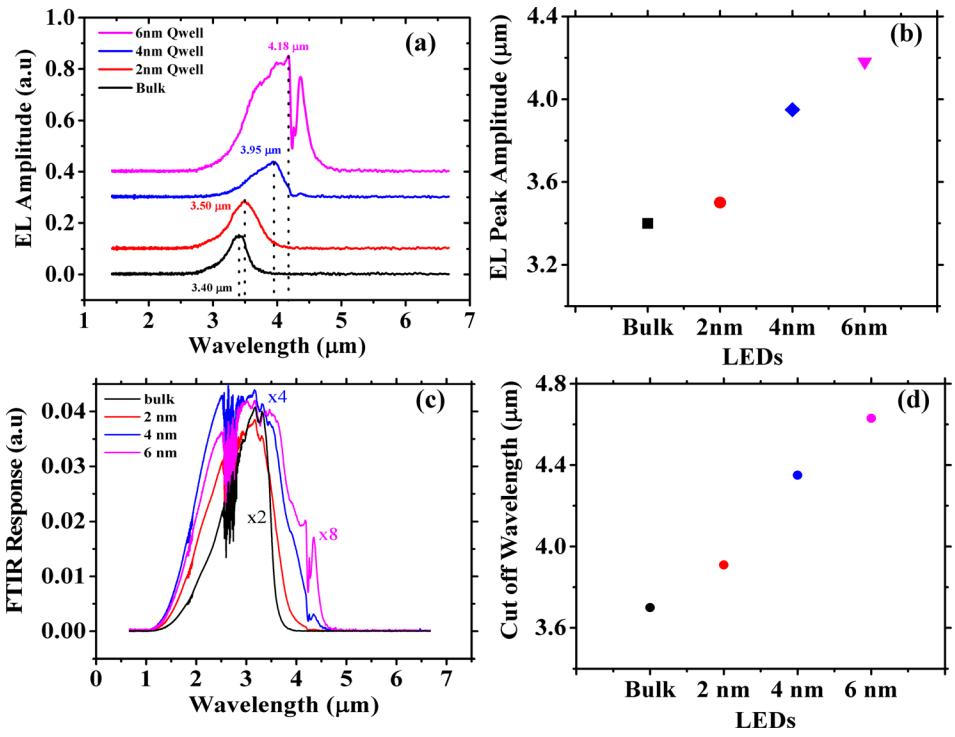

FIG. 3. (a) Electro-Luminescence spectra of bulk, 2 nm, 4 nm, and 6 nm LEDs at a forward current of 20 mA and (b) peak amplitude of each LED to highlight change in the peak position with the quantum well width. (c) FTIR photo response of bulk, 2 nm, 4 nm, and 6 nm LEDs at zero bias voltage with (d) all LEDs having different cut-offs can have application as the mid-IR-NIR (~1.3–4.6 μm) quantum well detector.

TABLE II. Comparison of measured and simulated emission wavelength of LEDs for three quantum-well widths.

	2 nm	4 nm	6 nm
Measured	3.5 μm	3.95 μm	4.18 μm
Simulated	3.7 μm	4 μm	4.3 μm

mixed trend: first a blue-shift up to 100 mA and then a red shift up to 160 mA. The 6 nm quantum well LED showed a slowly decreasing trend up to 100 mA of current. On the other hand, the bulk LED showed a consistent shift of the emission peak towards longer wavelength with any increase in the injection current. The blue-shift in the quantum well LEDs can be justified with the band filling effect in quantum well devices. The mixture of blue and red-shift could be attributed to a mixture of band filling and Joule heating effect.[18] At lower currents, the band filling dominates, but as the injection current increases, the LED temperature rises until thermal effects overcome band filling and an increase in wavelength is observed. However, the band filling is only observed in quantum well devices, as the bulk p-i-n LED shows a consistent peak-wavelength red shift with the injection current increasing, for any current measured. With regard to the full width at half maximum (FWHM), a broadening can be observed for all LEDs as the current increases, as shown in Fig. 4. The broadening of FWHM can also be attributed to the heat generation due to the same non-radiative processes which cause a red-shift in EL. However, as previously mentioned, non-radiative processes dominate in quantum well LEDs only at high currents, while the blue-shift in EL for lower current can be attributed to quantum wells states being filled.[19] The emission peak broadening in 4 nm and 6 nm QW can be attributed to well width fluctuations across individual well or well-to-well width fluctuations arising during QW growth.[20] Another possible source is the defects and spatial distribution of electrons and holes. Such defects can originate from the strain at the AlInSb/InSb interface, caused by increasing the well thickness from 2 nm to 4 nm and then to 6 nm. The strain hence induces fluctuations in confinement potential which in turn increase broadening.[15]

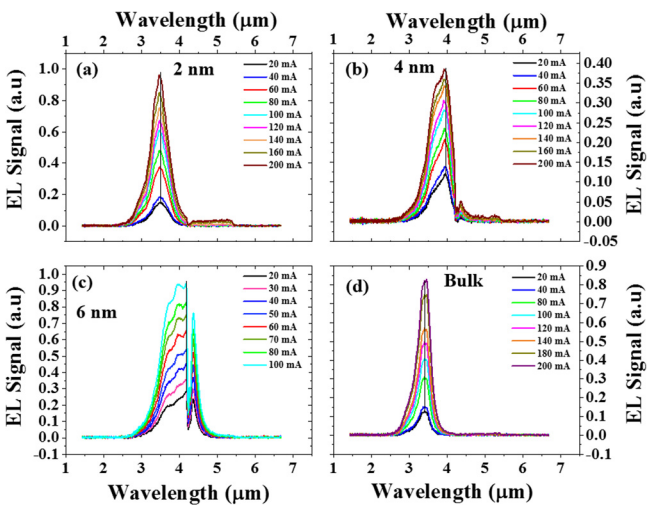

FIG. 4. The emission from each LED (a), (b), (c), and (d) measured at different forward injection currents.

In summary, four mid-IR LEDs based on bulk and three quantum well were grown monolithically on SI GaAs. The electroluminescence measurements show peak wavelength values consistent with the well widths, while photocurrent measurements at zero bias show the presence of photoresponse in the mid-IR. The EL in the range of forward currents measured suggests that emission from quantum well devices is due to filling and emptying of band states from the quantum well. This is a monolithically grown layer structure integrating four mid-IR LEDs on the same substrate. Based on current optimization, the same concept can be applied in a range of different material compositions to completely isolate each wavelength. The development of a multi-substance spectroscopic sensor employing monolithic IR sources and detectors is also possible with this concept. The FTIR response of LEDs indicates viability of these devices as infrared detectors covering a range (~1.3–4.6 μm) spanning from the NIR to the mid-IR. This wavelength range is of interest for detection of industrial gases and biological molecules for identification of diseases. The concept of a monolithic LEDs array exploiting an integrated switching device has great potential for applications in single chip multiple gas detections and electronically controlled multispectral infrared source/detector. The growth on SI GaAs wafers paves the way for switching architectures.

The authors would like to acknowledge the financial support from EPSRC under Grant Nos. EP/J018678/1 and EP/M01326X/1. The authors also wish to thank all the staff of James Watt Nanofabrication Centre (JWNC) at University of Glasgow for their assistance. The author M.A. would like to acknowledge Dr. Jorlandio F. Felix from University of Brisilia for his help with the IV data analysis. The authors also wish to acknowledge the trial version of SiLENSe software used for the simulations.

[1]D. Gibson and C. MacGregor, "A novel solid state non-dispersive infrared CO_2 gas sensor compatible with wireless and portable deployment," Sensors **13**, 7079 (2013).
[2]I. Ozden, E. Makarona, A. V. Nurmikko, T. Takeuchi, and M. Krames, "A dual-wavelength indium gallium nitride quantum well light emitting diode," Appl. Phys. Lett. **79**, 2532 (2001).
[3]R. C. Sousa, J. J. Sun, V. Soares, P. P. Freitas, A. Kling, M. F. da Silva, and J. C. Soares, "Large tunneling magnetoresistance enhancement by thermal anneal," Appl. Phys. Lett. **73**, 3288 (1998).
[4]S. Jung, S. Suchalkin, G. Kipshidze, D. Westerfeld, E. Golden, D. Snyder, and G. Belenky, "Dual wavelength GaSb based type I quantum well mid-infrared light emitting diodes," Appl. Phys. Lett. **96**, 191102 (2010).
[5]J. Wang, T. Zens, J. Hu, P. Becla, L. Kimerling, and A. M. Agarwal, "Monolithically integrated, resonant-cavity-enhanced dual-band mid-infrared photodetector on silicon," Appl. Phys. Lett. **100**, 211106 (2012).
[6]N. C. Das, "Infrared light emitting device with two color emission," Solid-State Electron. **54**, 1381 (2010).
[7]C. Xie, V. Pusino, A. Khalid, M. J. Steer, M. Sorel, I. G. Thayne, and D. R. S. Cumming, "Monolithic integration of an active InSb-based mid-infrared photopixel with a GaAs MESFET," IEEE Trans. Electron Devices **62**, 4069 (2015).
[8]C. Xie, V. Pusino, A. Khalid, M. Aziz, M. J. Steer, and D. R. S. Cumming, "A new monolithic approach for mid-IR focal plane arrays," Proc. SPIE **9987**, 99870T (2016).
[9]V. Pusino, C. Xie, A. Khalid, M. J. Steer, M. Sorel, I. G. Thayne, and D. R. S. Cumming, "InSb photodiodes for monolithic active focal plane arrays on GaAs substrates," IEEE Trans. Electron Devices **63**, 3135 (2016).
[10]N. C. Das, W. Chang, G. Simonis, and M. Tobin, "MWIR LED array for high-temperature target simulation," Proc. SPIE **6208**, 62080N (2006).
[11]M. Aziz, P. Ferrandis, A. Mesli, R. H. Mari, J. F. Felix, A. Sellai, D. Jameel, N. Al Saqri, A. Khatab, D. Taylor, and M. Henini, "Deep-level

transient spectroscopy of interfacial states in "buffer-free" p-i-n GaSb/GaAs devices," J. Appl. Phys. **114**, 134507 (2013).
[12]S. H. Huang, G. Balakrishnan, A. Khoshakhlagh, A. Jallipalli, L. R. Dawson, and D. L. Huffaker, "Strain relief by periodic misfit arrays for low defect density GaSb on GaAs," Appl. Phys. Lett. **88**, 131911 (2006).
[13]J. H. Werner, "Schottky barrier and pn-junction I/V plots- Small signal evaluation," Appl. Phys. A **47**, 291 (1988).
[14]M. Al-Suleiman, A. El-Shaer, A. Bakin, H.-H. Wehmann, and A. Waag, "Optical investigations and exciton localization in high quality $Zn_{1-x}Mg_xO$–ZnO single quantum wells," Appl. Phys. Lett. **91**, 081911 (2007).
[15]X.-Q. Lv, J.-Y. Zhang, L.-Y. Ying, W.-J. Liu, X.-L. Hu, B.-P. Z.-R. Qiu, S. Kuboya, and K. Onabe, "Well-width dependence of the emission linewidth in ZnO/MgZnO quantum wells," Nanoscale Res. Lett. **7**, 605 (2012).
[16]E. O. Göbel, H. Jung, J. Kuhl, and K. Ploog, "Recombination enhancement due to carrier localization in quantum well structures," Phys. Rev. Lett. **51**, 1588 (1983).
[17]G. Zhou and P. Runge, "Modeling of multiple-quantum-well p-i-n photodiodes," IEEE J. Quantum Electron. **50**, 220 (2014).
[18]J.-C. Su, S.-F. Song, and H.-S. Chen, "Chromaticity stability of phosphor-converted white light-emitting diodes with an optical filter," Appl. Opt. **50**, 177 (2011).
[19]Y. G. Seo, K. H. Baik, H. Song, J.-S. Son, K. Oh, and S.-M. Hwang, "Orange a-plane InGaN/GaN light-emitting diodes grown on r-plane sapphire substrates," Opt. Express **19**, 12919 (2011).
[20]T. G. Tenev, A. Palyi, B. I. Mirza, G. R. Nash, M. Fearn, S. J. Smith, L. Buckle, M. T. Emeny, T. Ashley, J. H. Jefferson, and C. J. Lamber, "Energy level spectroscopy of InSb quantum wells using quantum- well LED emission," Phys. Rev. B **79**, 085301 (2009).